Switching the aptamer attachment geometry can dramatically alter the signalling and performance of electrochemical aptamer-based sensors

Alejandro Chamorro-Garcia [a,b] , Gabriel Ortega [a,c], Davide Mariottini [b], Joshua Green [d] , Francesco Ricci[b] and Kevin W. Plaxco*[, a,d]

Electrochemical Aptamer-Based (EAB) sensors, comprised of an electrode bound DNA aptamer with a redox reporter on the distal end, offer the promise of high-frequency, real-time molecular measurements in complex sample matrices and even in vivo. Here we assess the extent to which switching the aptamer terminus that is electrode bound and the one redox reporter modified affects the performance of these sensors. Using sensors against doxorubicin, cocaine, and vancomycin as our test beds, we find that both signal gain and the frequency dependence of gain depend strongly on the attachment orientation, with 5'-anchored aptamers always exhibiting improved performance.

Because they are reagentless, single step, and able to work directly in highly complex sample matrices, electrochemical aptamer-based (EAB) sensors[1] support the convenient, high-frequency measurement of specific molecular targets both ex vivo in unprocessed clinical samples[2] and in situ in the living body[3]. Consisting of a redox-reporter-modified aptamer attached to an interrogating electrode surface, EAB sensors produce a signal when binding induces a conformational change in their target-recognizing aptamer. This in turn alters the electron transfer kinetics of the redox reporter, most often methylene blue (MB), which can be monitored electrochemically[4]. Given that this signalling mechanism is independent of the chemical or enzymatic reactivity of the sensor's target, EAB sensors are also generalizable[5], and can be adapted to new targets via the simple expedient of switching out their recognition aptamer. Consistent with this, EAB sensors have been reported for detection of a wide range of targets, including many proteins[6], inorganic ions[7], and small molecules[8]. Finally, due to their conformation-linked signalling, EAB sensors are highly selective and thus, as noted above, even support seconds-resolved, real-time molecular measurements in situ in the veins of living animals[3,9]. A number of design and "interrogation" (voltammetry) parameters have been described to date that affect the performance of EAB sensors[10]. For example, because EAB signalling is driven by binding-induced changes in electron transfer rate, their signal gain (relative signal change at saturating target) under square wave voltammetry (SWV) interrogation depends sensitively on the amplitude and frequency of the potential pulse employed[11]. We thus routinely tune both to achieve optimal sensor performance. Gain and, sometimes, affinity are likewise functions of the density with which the target-recognizing aptamer is packed onto its surface and thus we tune this parameter, too, in order to achieve optimal sensor performance[12]. Finally, to support either calibration free in vitro performance or drift-free in vivo performance we employ approaches that are reliant on the frequency-dependence of signal-gain, with this dependence also being a property that can also be optimized[13]. In addition to the above-described parameters, recent studies have also shown that the placement of the redox tag in an EAB sensor can significantly alter sensor performance[14]. In one study, for example, placement of the redox reporter at an internal position on the chain (i.e., not, as has most often been employed, at the distal terminus) was shown to *de*crease the gain of a sensor[15] for the detection of tumour necrosis factor alpha (TNF-α) by a factor of 2. Conversely, internal placement of the reporter in the aptamer sequence increased the gain of an insulin-detecting sensor[16] by a factor of 1.5. It is thus clear that redox-reporter placement can alter EAB sensor performance, albeit with the magnitude of any effects likely varying depending on the aptamer's structure and the details of the reporter's placement. Building on these observations, here we explored the extent to which switching which end of the aptamer is attached to the electrode and which is modified with the reporter alters the magnitude and frequency dependence of a sensor's gain. To do so we compared the performance of pairs of sensors in which the thiol group for anchoring the aptamer to the electrode is placed at the 5′ terminus and the redox reporter at the 3′ terminus with those in which this had been reversed (Fig. 1).

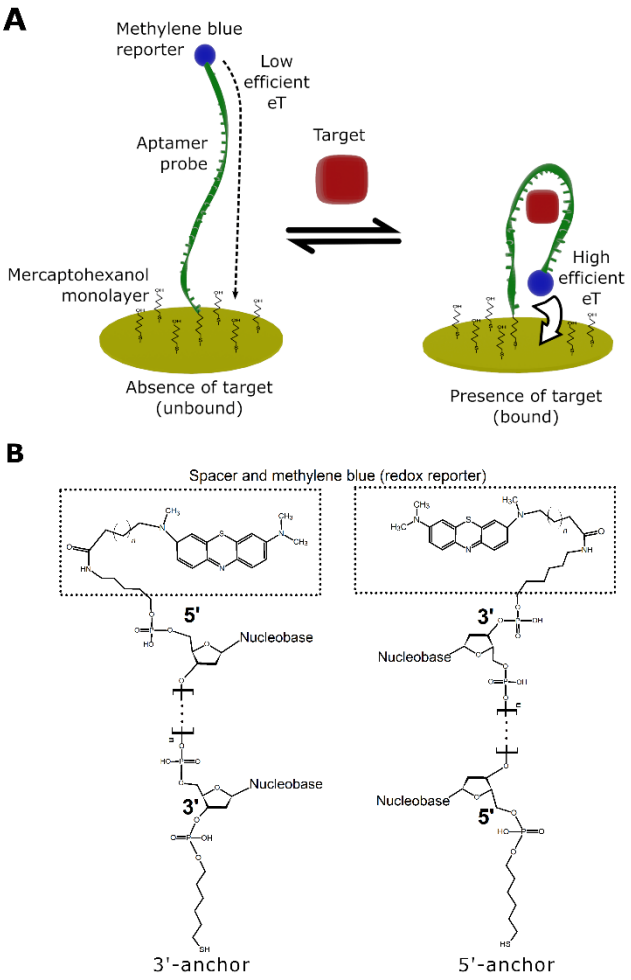

Figure 1. (A) Electrochemical aptamer-based (EAB) sensors are comprised of a target-binding aptamer attached via a thiol on one terminus to an interrogating electrode and modified, typically at the terminus distal to the electrode, with a redox reporter (here methylene blue: MB). Most reports of EAB sensors to date have anchored the aptamer to its interrogating electrode via its 5', with the redox reporter being situated on the 3' end. Here, however, we explore the extent to which the signalling properties of EAB sensors depend on this attachment orientation. (B) That is, we have explored the extent to which gain, the frequency dependence of gain, and target affinity vary when we switch the aptamer's attachment from its 3' end (left panel) to its 5' end (right panel).

As representative examples to explore the importance of this design parameter we have employed EAB sensors directed against the chemotherapeutic doxorubicin, the drug of abuse cocaine, and antibiotic vancomycin, all of which have previously been described using the commonly employed 5'-anchor (and thus 3' methylene blue) orientation[17]. Indeed, using this 5' attachment orientation, two of these sensors have been shown to support continuous, real-time measurements in situ in the living body[18]. Here, we explore the signal gain and affinity of these sensors as a function of the attachment orientation of their recognition aptamers and of the square-wave frequency employed in their interrogation. Please refer to supporting information for materials and methods and detailed description of the experimental procedures followed. Of note, the gain of EAB sensors is so strongly dependent on that latter parameter[11] that, at some frequencies, they exhibit signal-on behaviour (binding increases the signalling current), whereas at others they are signal-off. This simultaneous signal-on and signal-off behaviour serves as the basis for the most commonly employed drift correction algorithm used to ensure good EAB signal stability in vivo, and thus both behaviours are of importance.

The signalling characteristics of the doxorubicin-detecting sensor change quite significantly upon switching the aptamer's orientation. To see this, we characterized the gain of 3' and 5'-anchored sensors as a function of square wave frequency (Fig. 2A), finding that, while the highest signal-on gain we observe for the 5'-anchor orientation is 280±30% (unless otherwise noted, the confidence intervals here and elsewhere reflect the standard deviation of 4 replicates from independently fabricated sensors), at 700 Hz, the highest signal-on gain we obtained for the 3'-anchor orientation is only 85±13% (at 1,000 Hz). The highest magnitude signal-off gain we observed for the two constructs likewise differs, but to a lesser extent, being -35±10% for the 5'-anchor orientation (at 5 Hz) and -51±3% for the 3'-anchor orientation (at 10 Hz).

To ascertain whether the orientation effects on gain observed for the doxorubicin-binding aptamer hold for other aptamers, we next investigated sensors for the detection of either the drug-of-abuse cocaine (Fig. 2B) or the antibiotic vancomycin (Fig. 2C). Once again, we find that the attachment orientation affects signal gain of both. Specifically, while we observe 820±80% gain for the 5'-anchor orientation (at 900 Hz) of the cocaine-binding aptamer, the largest magnitude signal-on gain we observe for its 3'-anchor orientation is only 169±33% (at 430 Hz). For this sensor, neither orientation produced a signal-off response at any of the frequencies we investigated. Likewise, the vancomycin-detecting sensor reaches 61±4% signal-on gain (at 60 Hz) in its 5'-anchor orientation, but only 15±5% (at 50 Hz) in its 3'-anchor orientation, with signal-off gains of -38±2% (at 5 Hz) for the 5'-anchor orientation and -20±1% (at 5 Hz) for the 3'-anchor orientation. Thus, for all three of the sensors we have explored here, we observe significantly better gain (mainly in the signal-on frequency regime, but also to some extent in the signal-off frequency regime, see Figure S1 in supplementary information) for the 5'-anchor orientation. The generally strong frequency dependence of EAB signal gain has been used to perform drift correction for in vivo applications[3], and for producing calibration-free sensors[19]. This point is sufficiently important that, for those rare EAB sensors for which the gain is

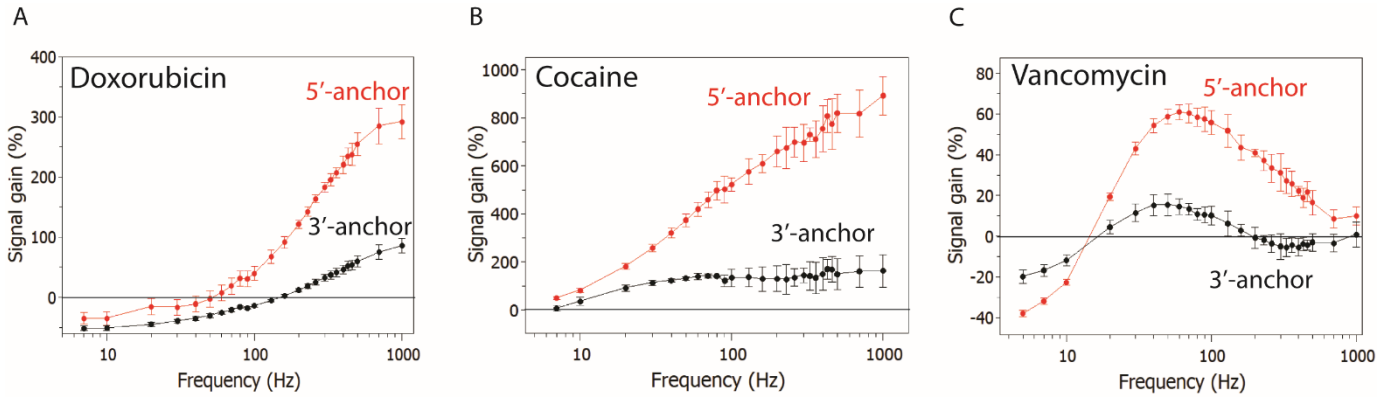

Figure 2. The signalling of electrochemical aptamer-based (EAB) sensors can be a strong function of the attachment orientation of their aptamers, but the extent to which it does varies depending on the aptamer. As shown here, for example, the signal gain of various EAB sensors, which is defined as the relative signal change between the absence of target and saturating target, varies strongly with the attachment orientation. Shown are plots of signal gain as a function of the square-wave interrogation frequency for (A) a doxorubicin-detecting sensor, (B) a cocaine-detecting sensor and (C) a vancomycin-detecting sensor. The error bars here and elsewhere in this paper denote the standard deviation of replicates collected using independently fabricated sensors. As saturating target concentrations we employed 100 µM, 7 mM or 100 µM in panels A, B, and C, respectively.

only weakly frequency dependent, we have developed new approaches to increasing the frequency dependence of EAB gain to ensure their good in vivo performance[20]. Given this, we note that, for the three sensors we have investigated here, the frequency dependence of their gain is, like their gain itself, also greater for their 5′ anchor orientations (Fig. 3).

In contrast to the effects of attachment geometry on signal gain, we do not a priori expect the affinity of the sensor (the mid-point of its binding response curve) to vary with the attachment geometry, as the aptamer's dissociation constant should not depend on which of its ends is attached to the surface. Consistent with this, we measured their binding curves (Fig. 4) and found that the affinity of each sensor remains effectively unchanged upon switching the anchoring orientation. The affinities' consistency allows us to foresee no discrepancies in selectivity or affinity in complex matrixes. However, this is an issue that needs to be addressed independently in each sensor's case and the specific scenario to be applied of application.

All three of the sensors explored here exhibit greater signal gain and stronger frequency-dependent gain when their aptamers are anchored via their 5′ termini. Consistent with this, previous studies employing electrode-bound, linear DNA strands to detect DNA hybridization likewise report greater gain for the 5′ anchor orientation[21]. Given this, we are tempted to speculate regarding the possible mechanistic origins of such an effect.

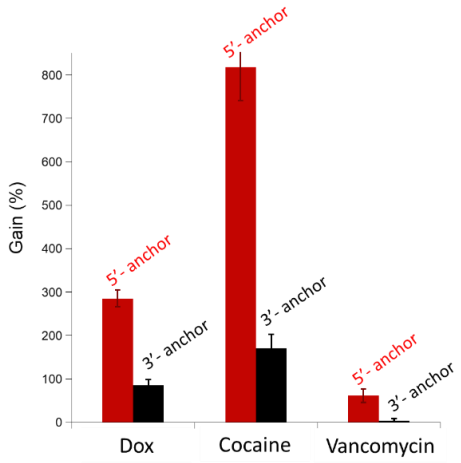

Figure 3. The more commonly used 5′ anchor orientation achieves notably higher gain (relative signal change in the presence of saturating target) for all three of sensor pairs we have investigated here. Shown here, for example, are the largest magnitude signal-on gains we observe for each sensor.

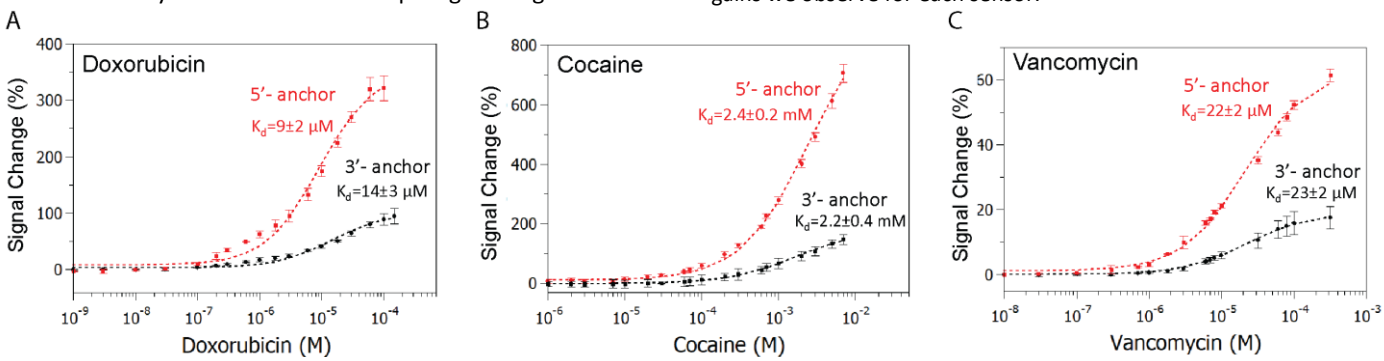

Figure 4: The affinities of the aptamers we have employed are independent of their attachment orientation. Specifically, in the 5′-anchor versus 3′-anchor orientations, we observe binding curve midpoints of 9±2 µM and 14±3 µM, respectively, for doxorubicin, (B) 2.4±0.2 mM and 2.2±0.4 mM for cocaine, and (C) 22±2 µM and 23±2 µM for vancomycin. Each curve employs the frequency at which the highest signal-on gain was recorded.

Specifically, it has previously been shown that short, double-stranded DNAs attached to a surface using a 5′ linkage adopt a more vertical orientation (relative to the surface) than those anchored via a 3′ linkage, leading to more rapid electron transfer from a reporter on the distal end of the latter[22]. This presumably arises due to subtle changes in the specific geometry of linkages to 3′ versus 5′ hydroxyl groups which, of course, are not equivalent. As all three of the aptamers we have explored here are thought to bring their two termini together in their bound, folded states, the portion of them closest to the electrode is likely also a double helix and thus likely also subject to this attachment-site orientation effect. This speculation aside, however, it is quite possible that, were we to characterize additional aptamers, we would find some that behave in the inverse manner, with the 3′ anchor orientation exhibiting higher gain and stronger frequency dependence. Fortunately, checking this empirically is simple and convenient.

Optimization of many of the parameters that define the fabrication and interrogation of EAB sensors have seen extensive study. The orientation with which the aptamer is anchored to the sensor surface, however, has not. Here we describe the effects and consequences of switching the attachment orientation using 3 well-established EAB sensors. Doing this we find that, while affinity remains unchanged for all three sensors, we observe significant differences in both their signal gain and its frequency dependence. In light of these observations, our "take-home message" is that: (1) attachment orientation can alter sensor function and (2) is a relatively easy parameter to investigate, suggesting that it should be explored in the optimization of new EAB sensors.

The authors declare the following competing financial interest(s): K.W.P. discloses service on the scientific advisory boards of Diagnostic Biochips Inc. and Nutromics, both of which are developing applications related to this work.

This work was supported by the NIH (R01AI145206). This project has received funding from the European Union's Horizon 2020 research and innovation programme under the Marie Sklodowska-Curie grant agreement No 799332.

References

1 C. Fan, K. W. Plaxco, A. J. Heeger, *Proc. Natl. Acad. Sci. U. S. A.* 2003, **100**, 9134– 9137; Y. Xiao, A.A. Lubin, A.J. Heeger, and K.W. Plaxco, *Angew. Chem.*, 2005, **44**, 5456-5459; Y. Xiao, R. Lai and K.W. Plaxco, *Nat. Protoc.,* 2007, **2**, 2875–2880; LR. Schoukroun-Barnes, Florika C. Macazo, B. Gutierrez, J. Lottermoser, J. Liu, and R.J. White, *Annual Review of Anal. Chem.,* **2016**, 9:1, 163-181.

2 J.S. Swenson, Y. Xiao, B.S. Ferguson, R.Y. Lai, A.J. Heeger, K.W. Plaxco and T.J. Soh, *J. Am. Chem. Soc.*, 2009, **131**, 4262–4266; R. J. White, H. M. Kallewaard, W. Hsieh, A.S. Patterson, J.B. Kasehagen, K.J. Cash, T. Uzawa, H. T. Soh, and K.W. Plaxco, *Anal. Chem.*, 2012, **84**, 1098-1103; A. Vallée-Bélisle, F. Ricci, T. Uzawa, F. Xia and K.W. Plaxco, *J. Am. Chem. Soc.*, **2012**, 134, 15197-15200; A. Idili, C. Parolo, G. Ortega and K.W. Plaxco, *ACS Sensors*, 2019, **4**, 3227-3233;

3 N. Arroyo-Currás, J. Somerson, P. Vieira, K. Ploense, T. Kippin and K.W. Plaxco, *Proc. Natl. Acad. Sci.*, 2017, **114**, 645-650; N. Arroyo-Curras, P. Dauphin-Ducharme, G. Ortega, K. Ploense, T. Kippin, and K.W. Plaxco, *ACS Sensors*, 2018, **3**, 360-366; A. Idili, N. Arroyo-Currás, K. L. Ploense, A. T. Csordas, M. Kuwahara, T. E. Kippin and K. W. Plaxco, *Chem. Sci.*, 2019, **10**, 8164-8170;

4 K.W. Plaxco, H.T. Soh, *Trends in Biotechnol.*, 2011, **29**, 1-5.

5 A. A. Lubin and K. W. Plaxco, *Accounts of Chem. Res.,* 2010, **43**, 496-505; L.R. Schoukroun-Barnes, C. F. Macazo, B. Gutierrez, J. Lottermoser, J. Liu and R. J. White, *Annu. Rev. Anal. Chem.,* **2016**, 9:1, 163-181.

6 Y. Xiao, A.A. Lubin, A.J. Heeger and K.W. Plaxco. *Angew. Chem.*, 2005, **44**, 5456-5459; Y. Xiao, B. D. Piorek, K. W. Plaxco and A. J. Heeger, *J. Am. Chem. Soc.*, 2005, **127**, 17990-17991.

7 Y. Wu and R. Y. Lai, *Biotechnol. J.*, 2016, **11**, 788-796.

8 B.R. Baker, R.Y. Lai, M. S. Wood, E. H. Doctor, A. J. Heeger and K. W. Plaxco, *J. Am. Chem. Soc.*, 2006, **128**, 3138-3139; A. Rowe, E. Miller and K. W. Plaxco, *Anal. Chem.*, 2010, **82**, 7090-7095.

9 P. Dauphin-Ducharme, K. Yang, N. Arroyo-Currás, K. Ploense, Y. Zhang, J. Gerson, M. Kurnik, T. E. Kippin, M. Stojanovic and K.W. Plaxco, *ACS Sensors*, 2019, **4**, 2832-2837.

10 M. Aller-Pellitero, A. Shaver and N. Arroyo-Curras*, J. Electrochem. Soc, 2*020, **167,** 037529.

11 R. J. White and K. W. Plaxco, *Anal. Chem.,* 2010, **82**, 73-76; P. Dauphin-Ducharme and K. W. Plaxco, *Anal. Chem.*, 2016, **88**, 11654-11662.

12 F. Ricci, Y. Lai, A. J. Heeger, K. W. Plaxco and J. J. Sumner, *Langmuir*, 2007, **23**, 6827-6834; R. J. White, K. W. Plaxco, *Langmuir*, 2008, **24**, 10513-10518; B.E. Fernández de Ávila, H.M. Watkins, J.M. Pingarrón, K.W. Plaxco KW, G. Palleschi and F. Ricci, *Anal. Chem.*, 2013, **85**, 6593–6597.

13 R. J. White and K. W. Plaxco, *Anal, Chem.*, 2010, **82**, 73-76; H. Li, P. Dauphin-Ducharme, G. Ortega, and K. W. Plaxco, *J. Am. Chem. Soc.*, 2017, **139**, 11207-11213.

14 A. A. Lubin, B. V. Stoep Hunt, R. J. White, and K. W. Plaxco, *Anal. Chem.*, 2009, **81**, 2150-2158; S.M. Silva, S. Hoque, V. R. Gonçales and J. J. Gooding, *Electroanalysis*, 2018, **30**, 1529-1535.

15 M. D. Mayer and R. Y. Lai, *Talanta*, 2018, **189**, 585-591.

16 J. Y. Gerasimov, C. S. Schaefer, W. Yang, R. L. Grout and R. Y. Lai, *Biosens. and Bioelectron.*, **42**, 2013, 62-68.

17 N. Arroyo-Currás, J. Somerson, P. A. Vieira, K. L. Ploense, T. E. Kippin and K. W. Plaxco, *Proc. Natl. Acad. Sci.*, 2017, **114**, 645-650; B. R. Baker, R. Y. Lai, M. S. Wood, E. H. Doctor, A. J. Heeger, and K. W. Plaxco, *J. Am. Chem. Soc.*, 2006, **128** (10), 3138-3139; P. Dauphin-Ducharme, K. Yang, N. Arroyo-Currás, K. L. Ploense, Y. Zhang, J. Gerson, M. Kurnik, T. E. Kippin, M N. Stojanovic, and K. W. Plaxco, *ACS Sensors*, 2019, **4**, 2832-2837.

18 N. Arroyo-Currás, J. Somerson, P. A. Vieira, K. L. Ploense, T. E. Kippin, K. W. Plaxco, *Proc. Natl. Acad. Sci.*, 2017, **114**, 645-650; P. Dauphin-Ducharme, K. Yang, N. Arroyo-Currás, K. L. Ploense, Y. Zhang, J. Gerson, M. Kurnik, T. E. Kippin, M N. Stojanovic, and K. W. Plaxco, *ACS Sensors*, 2019, **4**, 2832-2837.

19 H. Li, S. Li, J. Dai, C. Li, M. Zhu, H. Li, X. Lou, F. Xia and Kevin W. Plaxco, *Chem. Sci.*, 2019, **10**, 10843-10848.

20 A. Idili, N. Arroyo-Currás, K. L. Ploense, A. T. Csordas, M. Kuwahara, T. E. Kippin and K. W. Plaxco, *Chem. Sci.*, 2019, **10**, 8164-8170.

21 E. Farjami, R. Campos and E. E. Ferapontova. *Langmuir,* 2012, **28**, 16218-16226.

22 E. Farjami, R. Campos and E. E. Ferapontova. *Langmuir*, 2012, **28**, 16218-16226; M. Sam, E. M. Boon, J. K. Barton, M. G. Hill and E. M. Spain. *Langmuir*, 2001, **17**, 5727-5730.